Synchrotron x-ray scattering studies of semiconductor (111) surface reconstruction

I. K. Robinson[a)]
AT&T Bell Laboratories, Murray Hill, New Jersey 07974

(Received 29 July 1985; accepted 23 August 1985)

Some unifying principles of the mechanisms governing reconstruction at semiconductor surfaces will be discussed. Sources of synchrotron x-radiation are then shown to be an important asset in the problem of surface structure determination. Three recent examples of the application of x-ray diffraction techniques to semiconductor (111) surfaces will then be presented to illustrate the general remarks. (i) A structure determination of the InSb(111) surfaces shows very clear evidence of charge transfer leading to valence change in the top two layers of the structure. (ii) Structural analysis of the famous Si(111) 7×7 reconstructed is discussed in the light of certain models. (iii) A 7×7 state of Ge(111) seen in epitaxial films of Ge on Si(111) is attributed to compressive strain.

I. RECONSTRUCTION

This paper reviews recent applications of glancing incidence x-ray diffraction to the surface structure problem. This new technique promises to supercede low energy electron diffraction (LEED), the traditional method of determination, because the interpretation is much more straightforward. In particular, it allows *de novo* structure determination and avoids undue dependence on testing large numbers of model structures. The scope of the paper has been restricted to the discussion of Ge, Si, and InSb(111) surfaces and has been divided into sections accordingly.

Figure 1 shows a cartoon of an ideal (111) cut through a diamond lattice crystal to demonstrate that the one of the four covalent bonds of every surface atom "dangles" into the vacuum. This situation is undesirable in nature because of the large energy cost of the dangling bonds. To minimize its surface free energy, the crystal can employ a variety of mechanisms to rearrange the bonding. A necessary consequence of this reconstruction is that there is a *loss of symmetry*; the surface has lower symmetry than the bulk. Loss of local point group symmetry leads to displacements of atoms from special positions in the crystallographic unit cell. Loss of translational symmetry leads to a superstructure in which the surface unit cell is a multiple (usually integral) of that of the truncated bulk. The latter is a common occurrence and thus the notation "$n\times m$ reconstruction" is used to designate the size of the new unit cell as a multiple of the bulk in the two principal directions. Some of the more important of these mechanisms are listed below, and examples are given where appropriate. Emphasis is placed on the impact of each mechanism on the atomic geometry, and how knowledge of the surface structure can identify the mechanism.

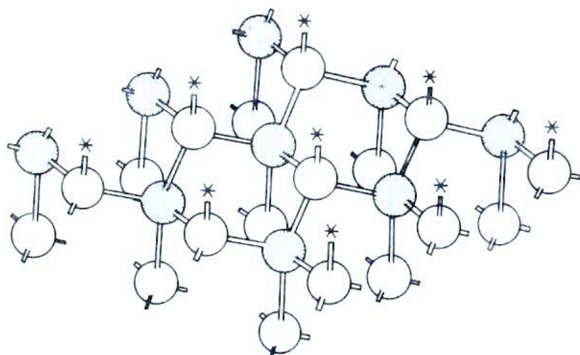

FIG. 1. Ball and stick model of the zinc blende structure exposing a (111) surface to the vacuum (top). Dangling bonds at the surface are marked (*). For the InSb(111) surface, In atoms (unshaded) occupy the topmost layer, with Sb atoms (shaded) beneath; the InSb($11\bar{1}$) surface has the labels reversed. Ge and Si have the diamond structure, identical in its atomic positions but without differentiation of atom types.

1. Dimerization. Dangling bonds can pair up to form bridging bonds between the surface atoms. Substantial subsurface relaxation is then needed to help restore the bond angles and lengths to the sp^3 tetrahedral arrangement. Dimerization is therefore evident in displacements of atoms to new positions separated by a covalent bond length. This mechanism is known to occur in the Ge(100) 4×2 and Si(100) 4×2 reconstructed surfaces.[1]

2. π-bond formation. Another way to relieve dangling bonds is to form double bonds in place of single ones. This has two consequences observable in the atomic positions: the bond lengths become shorter and the bond angles at the participating atoms approach sp^2 coordination values. π bonding is believed to be the mechanism for the 2×1 reconstruction of the cleaved C, Si, and Ge(111) surfaces, apparent in the unusual optical and electrical properties of these surfaces.[2]

3. Valence change. Electron transfer to or from a surface atom will change the number of covalent bonds it forms. It also changes the bond angles of the remaining bonds so that its presence is detectable in the surface structure. The electron transfer would either charge or (in the case of the III–V semiconductors) discharge the surface, and this may enter the energy balance to favor or disfavor reconstruction. Known examples are the (110) and (111) surfaces of GaAs.[3,4]

4. Stoichiometry change. In this general class, we include the addition of extra atoms ("adatoms"), deletion of atoms (vacancy formation), and substitution of one atom type for another in the surface layer or layers. Vacancy formation is known to be involved with the reconstruction of GaAs(111)[4] and InSb(111) as described below. Adatoms are a central part of certain models of the famous Si(111) 7×7 reconstruction[5–7] (also discussed below) but this struc-

 0734-2101/86/031309-06$01.00 © 1986 American Vacuum Society

ture is still far from being solved and is the subject of much debate.[8]

5. Topological changes. The bonding among atoms several layers below the surface can rearrange entirely in the most general kind of reconstruction. The diamond structure has only six-membered rings of atoms, but a topological reconstruction would have other sizes, five- and seven-membered rings, for instance. Many of the models of the Si(111) 7×7 reconstruction have this feature.

It is clear that the best way to distinguish among these and other possible mechanisms of reconstruction is accurate structural analysis, preferably placing atoms within 0.01 Å. Ultimately, general principles will emerge from the study of many examples. It is already clear that polymorphism and metastability are present in such systems [e.g., Si(111) 2×1 or 7×7]. It is also known that the reconstructed state of a surface can depend on temperature[9] and lateral pressure (see below); the physics of phase transitions in these two-dimensional systems is largely unexplored.

II. GLANCING INCIDENCE X-RAY DIFFRACTION

Historically, the greatest efforts in the study of reconstructed surface structures have been made by LEED. Most of the examples above have been studied using this technique. Experimentally, intensity measurements are made of beams of electrons backreflected from a crystal surface as a function of energy, i.e., wavelength. The 10–300 eV electrons penetrate 10 Å or so into the surface, providing sensitivity to that part of the crystal. The most important drawback of the technique is that structure factor calculations are made very difficult by uncertainties of the form factor and by multiple scattering; this greatly limits the ability of the technique to distinguish between models of a surface, let alone solve them *ab initio*.

The advent of intense, bright sources of x-ray synchrotron radiation may allow x-ray crystallography to replace its electron analog by permitting the use of straightforward linear superposition (e.g., Fourier) methods of analysis with which there exists a large body of experience. The need for intensity is shown in Table I, where counting rates for diffraction from crystalline monolayers are calculated (using the Thomson formula) as a function of source. Experiments are just on the verge of feasibility with the most intense "conventional" sources,[10] but only become straightforward when storage ring sources are used.

TABLE I. Incident and calculated diffracted intensity (in photons/s) from a hexagonal close packed monolayer of Au or Si as a function of x-ray source. When more dilute layers of atoms (such as in reconstructed surfaces) are considered, the intensity becomes very much smaller; in a primitive structure, it varies as the inverse fourth power of the unit cell edge.

	Incident	Diffracted from	
		Au($Z=79$)	Si($Z=14$)
60 kW rotating anode	10^8	10	10^{-2}
SSRL bending magnet (focused)	10^{12}	10^6	10^3
SSRL wiggler (focused)	10^{13}	10^7	10^4
6 GeV undulator (estimated)	10^{16}	10^{10}	10^7

To obtain the numbers in Table I, it was necessary to make certain assumptions about the instrument and diffraction geometries. X-ray diffractometers are customarily optimized to provide high resolution in the diffraction plane, but to trade off resolution for flux in the out-of-plane direction. This asymmetry of the resolution function can exceed 200:1. The diffraction pattern of a reconstructed surface is highly diffuse in the direction perpendicular to the surface, so this direction has to be placed along the poor resolution direction to optimize flux and to not compromise instrumental resolution. This geometry is called "glancing incidence" because the incident and diffracted x-ray beams both make small angles with the surface. A small, nonzero component of perpendicular momentum transfer ($q_\perp$) is customarily used to avoid problems of refraction at the surface; since the diffraction intensity is slow varying in this direction, the measured intensity approximates the value at $q_\perp = 0$ quite well.

The typical instrument used for such measurements is shown in Fig. 2. It consists of a four-circle diffractometer with its axis horizontal for used with synchrotron radiation sources.[11] The plane of the sample, parallel to the diffraction plane, is vertical. The sample moves on a goniometer inside a stainless steel ultrahigh vacuum (UHV) system that sits beside the diffractometer. The coupling through the vacuum wall involves bellows and a doubly differentially pumped rotating seal.[11] Such instruments in various stages of design and construction are becoming associated with most of the synchrotron radiation facilities of the world.

III. InSb(111) 2×2 SURFACE

The (111) and $(11\bar{1})$ surfaces of this III–V compound have 2×2 and 3×3 reconstructions, respectively, when prepared in UHV by ion bombardment and thermal annealing. The reason for the difference in surface unit cell size is that these faces are polar, as Fig. 1 demonstrates: the topmost layer of the (111) face contains only In atoms, the second only Sb; the $(11\bar{1})$ face has the order reversed.

Synchrotron diffraction data were collected at HASYLAB, Hamburg using x rays from the storage ring DORIS. The data of the (111) 2×2 surface[12] and the $(11\bar{1})$ 3×3 surface[13] have been presented previously. The (111) 2×2 data were analyzed by means of the Patterson (pair-correlation) function shown in Fig. 3(a): this is the two-dimensional Fourier transform of the fractional order intensities sampled near $q_\perp = 0$ and corrected for polarization, Lorentz factor, and sample area. Integer order reflections were suppressed because of possible interference by diffraction from the bulk crystal underneath. Figures 3(b) and 3(c) show how a simple distortion of a ring of six atoms, which would form a regular hexagon in a (111) projection of the bulk structure, can explain the three nonorigin peaks of the Patterson. This arrangement of atoms is the only simple one that agrees, while maintaining 3 m symmetry. It is not, however, a complete description of the structure; more information can be obtained using the difference Fourier technique[12] or by comparing structure factors calculated from simple two-dimensional models of the surface, as Fig. 4 demon-

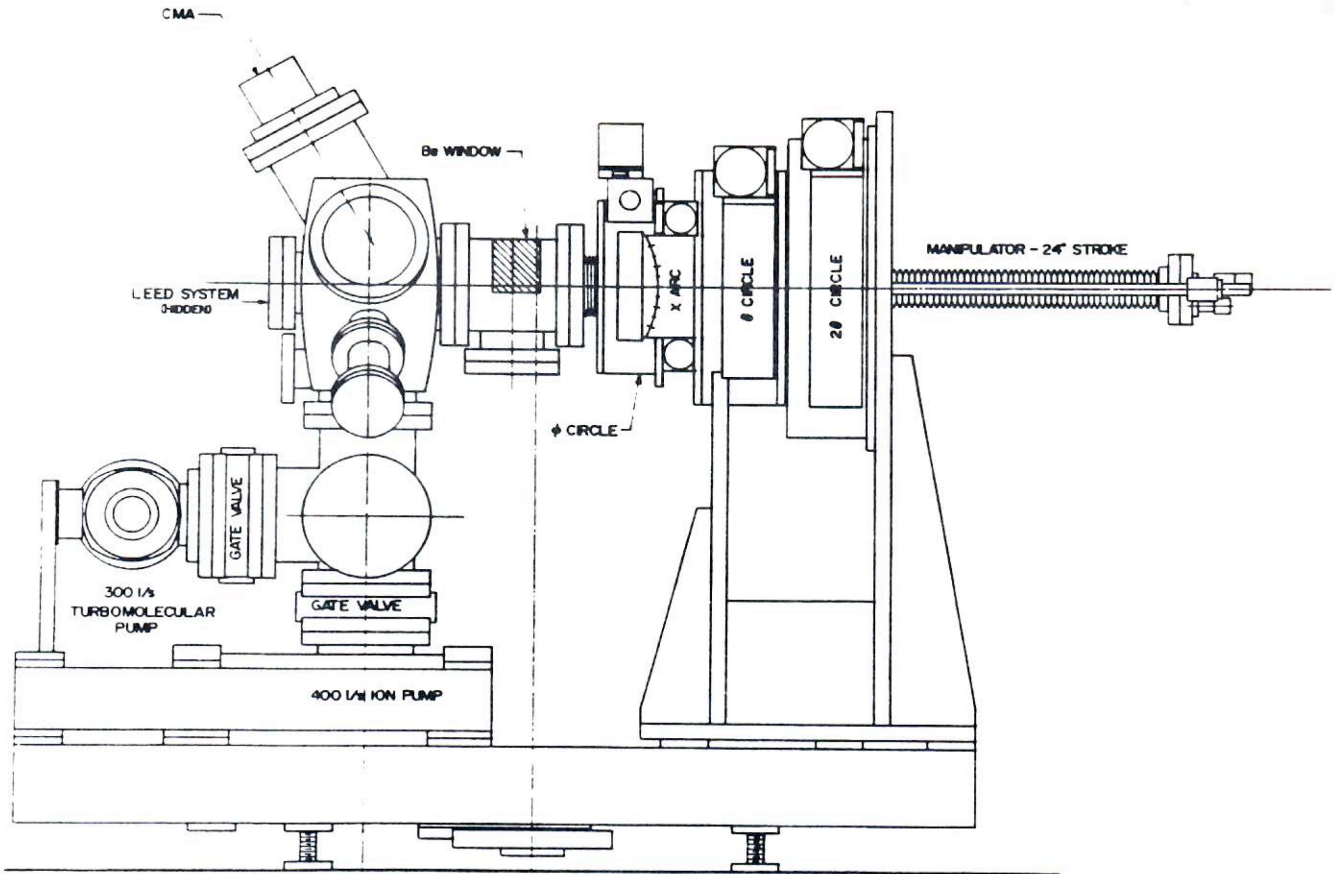

FIG. 2. Instrument used to measure glancing incidence x-ray diffraction from a surface in ultrahigh vacuum (Ref. 11). The diffractometer is on the right and the vacuum system on the left. In the center is a beryllium window through which x rays enter and leave the vacuum.

strates. The former is a model independent method that has been described previously[12]; the model testing approach in the figure vividly demonstrates the sensitivity of the x-ray data. The χ^2 values stated represent the level of disagreement between calculated (F_j^{calc}) and observed (F_j^{obs}) structure factors on an absolute scale

$$\chi^2 = \frac{1}{N} \sum_{j=1}^{N} \frac{(|F_j^{\text{calc}}| - F_j^{\text{obs}})^2}{\sigma_j^2}.$$

The σ_j's are the experimental errors in the N observations.

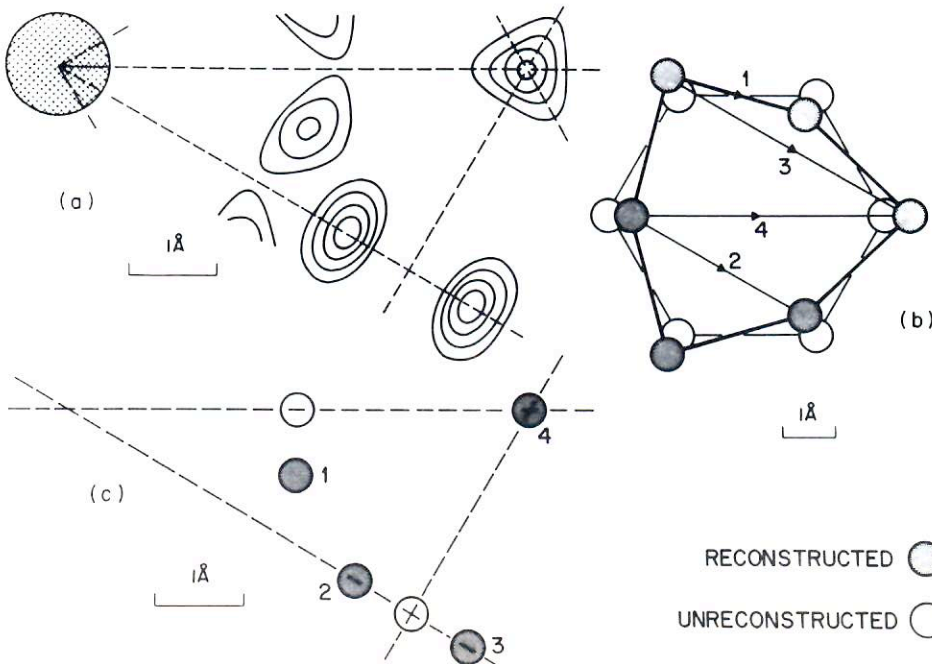

FIG. 3. (a) Positive contours of the Patterson function for InSb(111) 2×2. (b) Distortion of a hexagon (open circles) to an arrangement of atoms consistent with the Patterson (shaded circles). (c) Positions of Patterson peaks 1–4 from the structures in (b).

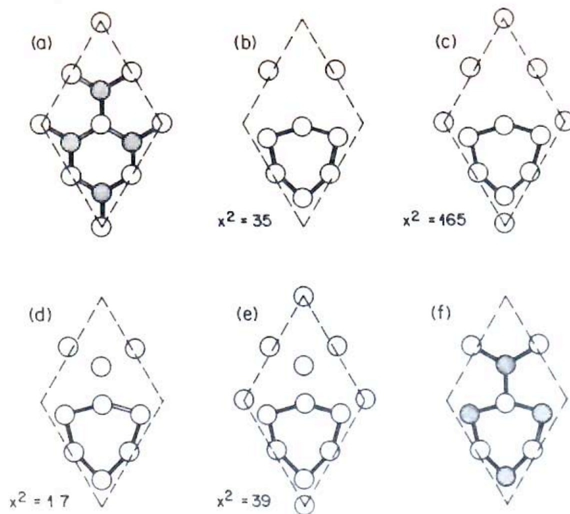

FIG. 4. (a) Unreconstructed 2 × 2 unit cell of InSb(111). The group V elements (Sb, shaded) are in the second layer. (b) Distorted hexagon arrangement (derived from Fig. 3) installed in a 2 × 2 unit cell. χ^2 is a least squares measure of misfit of calculated structure factors with observed. (c), (d), (e) Ditto with extra atoms added in high symmetry positions. (f) Final structure with assignment of atom types and bonds.

Thus, when χ^2 drops to the order of unity, the discrepancies are entirely accounted for by errors of measurement, and no further information can be obtained by improving models.

Figure 4(b) shows that the six atom arrangement of the distorted hexagon is actually a poor one, and clearly provides an inadequate description of the observations. However, when one more atom is added, χ^2 drops to a value of 1.7 showing good agreement. Other arrangements, including those with different numbers of atoms, fit badly as the figure shows. We can conclude that the seven atom description is the only simple possibility. We have direct evidence, therefore, for the existence of a *vacancy* in the InSb(111) 2×2 surface, since a unit cell without reconstruction would contain a multiple of four atoms. Two layers (four In and four Sb atoms in the unit cell) are reconstructed with one atom missing. Because In and Sb are isoelectronic in InSb, it is difficult to distinguish between them crystallographically; the close structural similarity with the GaAs(111) 2×2 reconstructed surface studied with LEED,[4] however, allows us to conclude there is an In vacancy in the top layer. The designation of atom types and bonds in Fig. 4(f) reflects this assumed similarity.

At the present stage of refinement, atoms are positioned with an accuracy of ± 0.05 Å. From the fact that the *two projected* In–Sb bond lengths (2.87 and 2.82 Å) are within error of (but actually slightly longer than) the bulk bond length of 2.81 Å, we can see immediately that the structure is rather flat. This is again in agreement with LEED structure of GaAs(111) 2×2, which is flat to within 0.11 Å. From the bond length we see no evidence of π bonding in the surface. In-plane bond angles are also meaningful even though we have only two-dimensional data because the structure is so flat. The three Sb atoms in the hexagon have an in-plane angle of 96° (and two angles of ≈90° to the bond connecting the layer below). Thus, these Sb atoms are showing a tendency to form *p*-like bonds (octohedral) instead of sp^3 bonds (tetrahedral) in the bulk, precisely the behavior expected for *trivalent* Sb. The bond angle in $SbBr_3$ is 95° by comparison. The expected trend down the Periodic Table from As to Sb towards more octohedral bonding is correctly demonstrated by the LEED value of 104° (in-plane) at the corresponding As in GaAs(111) 2×2.[4]

IV. Si(111) 7×7 SURFACE

A homopolar semiconductor is likely to use a reconstruction mechanism (or mechanisms) from the list in Sec. I that is different from a compound material in which the covalent bonds between unlike atoms are stronger than those between like ones. Numerous possible structures have been proposed for Si(111) 7×7 to explain a variety of known physical and chemical properties of the surface.[8] Given the complexity of the surface implied by the large unit cell size, it seems that only a technique that provides a larger amount of mutually orthogonal data could be expected to solve the structure unambiguously. To obtain ~100 sets of atomic coordinates for a structure four layers deep (see Fig. 1), in principle, requires ~300 independent measurements. Stereochemical constraints and symmetry will reduce this number but do not necessarily lend themselves simply to be incorporated in the analysis; besides, some redundancy would be desirable too. Of the available experimental techniques, only diffraction methods meet the criterion. LEED calculations, hard for small structures as explained above, are totally impractical (at present) for this application. We are only left with two techniques: high energy transmission electron diffraction[7,14] (TED) and x-ray diffraction. The high electron energies involved with TED serve to avoid the form factor and multiple scattering problems and render the structure factors directly comparable with x-ray ones.

Work is in progress with both methods at the moment. Our x-ray diffraction data measured on beamline VII-2 at Stanford Synchrotron Radiation Laboratory (SSRL)[15] are shown pictorially in Fig. 5; this format facilitates comparison with other published work[7,14,16] and reflects the general level of reproducibility (self-consistency) so far obtained. Visual comparison of these with published TED data[7,14] shows striking agreement; our data agree as well with these as do the two independent TED measurements[7,14] with each other. This suggests that TED is behaving in a truly kinematical fashion in this application, at least to the level of accuracy so far obtained. We have shown a two-dimensional asymmetric unit of the data assuming 6 mm symmetry. This is correct only for the $q_\perp = 0$ section of a three-dimensional data set because of the center of symmetry; the surface structure is known to have *at most* 3 m symmetry from scanning tunneling electron (STM) images.[5] TED cannot break the ambiguity, always seeing 6 mm symmetry since the electron beam necessary passes through both (111) and $(\overline{1}\overline{1}\overline{1})$ surfaces in the transmission geometry. We expect to see a breaking of 6 mm symmetry in our measurements at sufficiently large $q_\perp$, but a systematic search will require more beam time.

The Patterson (pair correlation) function is contoured in Fig. 5(b). The atomic positions of a double layer of unreconstructed silicon is superimposed. This map has not yet been fully interpreted, but the main feature is very clear: a sole

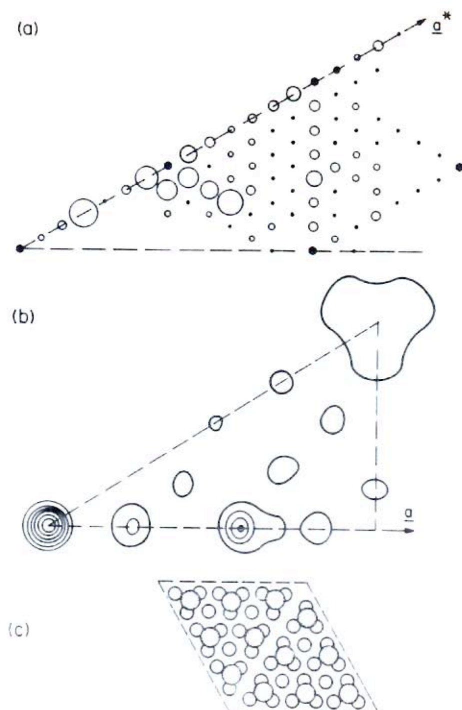

FIG. 5. (a) Observed diffraction data for Si(111) 7×7. The area of each circle is proportional to the measured intensity. Unmeasured reflections remain blank; dots represent statistically insignificant measurements. (b) Patterson function calculated from (a). (c) A structure consistent with the diffraction data. Two layers of atoms are superimposed; the unshaded layer contains a "stacking fault island," (Ref. 17) while the shaded one corresponds to the positions of the bumps in scanning tunneling images (Ref. 5).

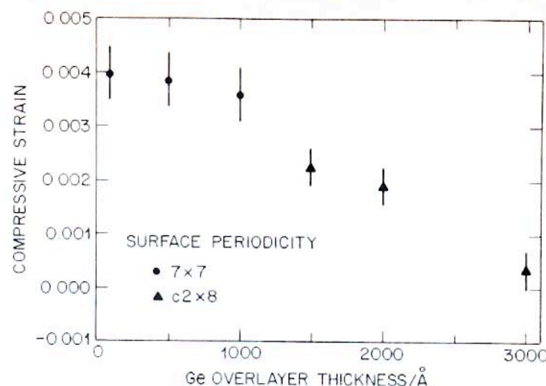

FIG. 6. Compressive strain $\epsilon = (a_{Ge} - a_{film})/a_{film}$, as a function of film thickness for Ge epitaxial films grown on Si(111) substrates. a_{film} and a_{Ge} are the film and bulk Ge lattice constant, respectively. The symbols indicate the reconstructed state seen after cooling the sample.

strong peak at interatomic vector (2,0) implying a strong periodicity in the structure with twice the bulk spacing. This is in good agreement with STM pictures[5] and also with analysis of low energy ion scattering data.[6] The absence of (4,2) or higher order peak tells us that the structure is *not* a pseudo 2×2 arrangement, but must have only small patches with this spacing. Instead, the arrangement in Fig. 5(c) which combines the principle of a "stacking-fault island," suggested by Bennett *et al.*[17] with 12 atoms in two antiphase triangles of 6, as suggested by both Binnig *et al.*[5] and Aono *et al.*[6] agrees well with the data.[15]

V. Ge(111) 7×7 STATE

This last section concerns more general aspects of reconstruction, unrelated to specific structural details, but shows how glancing incidence x-ray diffraction can be applied to the study of thin films. Here, the principal advantage is neither the monolayer sensitivity nor the kinematical behavior, but the high resolution and high absolute accuracy. The effects we examine involve perturbations in the lattice parameter of Ge by less than half a percent.

It is well known[18] that thin ($< 1\,\mu$m) epitaxial films of one crystal upon another of slightly different lattice parameter can exhibit lateral strain, often as large as a few percent. This is possible because the elastic energy in such a film (which scales as the thickness) can be comparable to the energy required to form misfit dislocations at the interface.[19] Since epitaxial films have a well-defined free surface exposed to the UHV conditions of their growth, and contamination levels are of necessity low, it is a reasonable question to ask how the strain affects the reconstruction of the surface.

The answer for the case of Ge grown on Si(111) substrates is shown in Fig. 6. The film strain, measured directly from the position of the in-plane film ($\bar{4}22$) Bragg reflection is plotted against the thickness. The Ge is compressed slightly so that its lattice parameter is closer to that of the Si substrate (4% different in lattice parameter); the single crystal quality of the films is good with mosaic spreads less than 0.5°. Halfway across this thickness/strain curve, at a critical strain between 0.22% and 0.34%, the reconstructed state switches abruptly from the customary 2×8 reconstruction to a new 7×7 one, seen for the first time in these experiments.[20]

The Ge(111) 7×7 state appears from LEED and ion channeling[21] as well as STM studies[22] to be isomorphic with the Si(111) 7×7 discussed above. This has great significance for the actual mechanism of reconstruction, implicating the role of lateral stress forces in these structures. Strain is clearly involved with the InSb(111) 2×2 surface described above; the reconstructed layers have 7 atoms in place of 8, which displace to spread themselves uniformly over the surface, partially filling in the vacancy (see Fig. 4). The 7×7 model of Fig. 5(c) also incorporates the strain principle in an elegant way; the faulted layer contains 42 atoms instead of 49 (in an unfaulted layer), directly displaying a 7% strain. It is gratifying to see that the apparent difference in reconstructed state between Ge(111) and Si(111), whose surface properties are otherwise very similar, can now be considered as due to a slight perturbation of lattice parameter.

ACKNOWLEDGMENT

We would like to thank HASYLAB and SSRL for support and assistance with the synchrotron radiation experiments.

[a] Experimental results obtained in collaboration with J. Bohr, R. Feidenhansl, M. Nielsen, and M. Toney, at Riso National Laboratory, Denmark; R. L. Johnson, MPI Stuttgart; H. J. Gossmann, J. C. Bean, L. C. Feldman, E. G. McRae, P. H. Fuoss, J. Stark, and W. Waskiewicz, AT&T Bell Labs; P. A. Bennett, Arizona State University.

[1] F. Jona, H. D. Shih, D. W. Jepsen, and P. M. Marcus, J. Phys. C. **12**, L455 (1979); P. Eisenberger, and W. C. Marra, Phys. Rev. Lett. **46**, 1081 (1981).
[2] K. C. Pandey, Phys. Rev. Lett. **47**, 1913 (1983); **49**, 223 (1982).
[3] A. R. Lubinsky, C. B. Duke, B. W. Lee, and P. Mark, Phys. Rev. Lett. **36**,

1058 (1976); S. Y. Tong, A. R. Lubinsky, B. J. Mrstik, and M. A. van-Hove, Phys. Rev. B **17**, 3303 (1978).
[4]S. Y. Tong, G. Xu, and W. N. Mei, Phys. Rev. Lett. **52**, 1693 (1983); D. J. Chadi, *ibid.* **52**, 1911 (1983).
[5]G. Binnig, H. Rohrer, C. Gerber, and E. Weibel, Phys. Rev. Lett. **50**, 120 (1983).
[6]M. Aono, R. Souda, C. Oshima, and Y. Ishizawa, Phys. Rev. Lett. **51**, 801 (1983).
[7]K. Takayanagi, J. Microsc. **136**, 287(1984); J. C. H. Spence, Ultramicrosc. **11**, 117 (1983).
[8]R. M. Tromp and E. J. van Loenen, Surf. Sci. **155**, 441 (1985), and references therein.
[9]P. A. Bennett and M. B. Webb, Surf. Sci. **104**, 74 (1980); I. K. Robinson, in *Proceedings of the 1st International Conference on the Structure of Surfaces* (Springer, Berlin, 1984).
[10]P. M. Eisenberger and W. C. Marra, Phys. Rev. Lett. **46**, 1080 (1981); I. K. Robinson, *ibid.* **50**, 1145 (1983).
[11]P. H. Fuoss and I. K. Robinson, Nucl. Instrum. Methods **222**, 171 (1984).
[12]J. Bohr, R. Feidenhans'l, M. Nielsen, M. Toney, R. L. Johnson, and I. K. Robinson, Phys. Rev. Lett. **54**, 1275 (1985).
[13]R. L. Johnson, J. H. Fock, I. K. Robinson, J. Bohr, R. Feidenhans'l, J. Als Nielsen, M. Nielsen, and M. Toney, in *Proceedings of the 1st International Conference on the Structure of Surfaces* (Springer, Berlin, 1984).
[14]E. G. McRae and P. M. Petroff, Surf. Sci. **147**, (1984).
[15]I. K. Robinson, W. K. Waskiewicz, P. H. Fuoss, J. B. Stark, and P. A. Bennett (in preparation).
[16]E. G. McRae, Surf. Sci. **147**, 385 (1984).
[17]P. A. Bennett, L. C. Feldman, Y. Kuk, E. G. McRae, and J. E. Rowe, Phys. Rev. B **28**, 3656 (1983).
[18]G. C. Osbourn, Phys. Rev. B **27**, 5126 (1983).
[19]F. C. Frank, and J. J. van der Merwe, Proc. R. Soc. A **198**, 205 (1949); **198**, 216 (1949).
[20]H. J. Gossman, J. C. Bean, L. C. Feldman, E. G. McRae, and I. K. Robinson, J. Vac. Sci. Technol. A **3**, 1633 (1985).
[21]H. J. Gossman, J. C. Bean, L. C. Feldman, E. G. McRae, and I. K. Robinson, Phys. Rev. Lett. **55**, 1106 (1985).
[22]R. S. Becker, J. A. Golovchenko, and B. S. Swartzentruber, Phys. Rev. Lett. **54**, 2678 (1985).